This article was downloaded by: [Renmin University of China]
On: 13 October 2013, At: 11:34
Publisher: Taylor & Francis
Informa Ltd Registered in England and Wales Registered Number: 1072954 Registered office: Mortimer House, 37-41 Mortimer Street, London W1T 3JH, UK


Advanced Composite Materials
Publication details, including instructions for authors and subscription information:
http://www.tandfonline.com/loi/tacm20

# Damage accumulation behavior of non-crimp fabric-reinforced epoxy composite under static and cyclic tensile loading

T. Sakai [a], S. Wakayama [a], E. Pérez-Pacheco [b], J. Rodriguez-Laviada [c] & C.R. Rios-Soberanis [a c]

[a] Department of Mechanical Engineering, Tokyo Metropolitan University, Hachioji, Japan

[b] Instituto Tecnológico Superior de Calkiní en el Estado de Campeche, Campeche, Mexico

[c] Centro de Investigación Científica de Yucatán, Unidad de Materiales, Merida, Mexico

Published online: 20 Jun 2013.

To cite this article: T. Sakai, S. Wakayama, E. Pérez-Pacheco, J. Rodriguez-Laviada & C.R. Rios-Soberanis (2013) Damage accumulation behavior of non-crimp fabric-reinforced epoxy composite under static and cyclic tensile loading, Advanced Composite Materials, 22:4, 281-297, DOI: 10.1080/09243046.2013.809636

To link to this article: http://dx.doi.org/10.1080/09243046.2013.809636

PLEASE SCROLL DOWN FOR ARTICLE

Taylor & Francis makes every effort to ensure the accuracy of all the information (the "Content") contained in the publications on our platform. However, Taylor & Francis, our agents, and our licensors make no representations or warranties whatsoever as to the accuracy, completeness, or suitability for any purpose of the Content. Any opinions and views expressed in this publication are the opinions and views of the authors, and are not the views of or endorsed by Taylor & Francis. The accuracy of the Content should not be relied upon and should be independently verified with primary sources of information. Taylor and Francis shall not be liable for any losses, actions, claims, proceedings, demands, costs, expenses, damages, and other liabilities whatsoever or howsoever caused arising directly or indirectly in connection with, in relation to or arising out of the use of the Content.

This article may be used for research, teaching, and private study purposes. Any substantial or systematic reproduction, redistribution, reselling, loan, sub-licensing,

systematic supply, or distribution in any form to anyone is expressly forbidden. Terms & Conditions of access and use can be found at http://www.tandfonline.com/page/terms-and-conditions

Downloaded by [Renmin University of China] at 11:34 13 October 2013

*Advanced Composite Materials*, 2013
Vol. 22, No. 4, 281–297, http://dx.doi.org/10.1080/09243046.2013.809636

Taylor & Francis
Taylor & Francis Group

# Damage accumulation behavior of non-crimp fabric-reinforced epoxy composite under static and cyclic tensile loading

T. Sakai[a]*, S. Wakayama[a], E. Pérez-Pacheco[b], J. Rodriguez-Laviada[c] and C.R. Rios-Soberanis[a,c]

[a]*Department of Mechanical Engineering, Tokyo Metropolitan University, Hachioji, Japan;*
[b]*Instituto Tecnológico Superior de Calkiní en el Estado de Campeche, Campeche, Mexico;*
[c]*Centro de Investigación Científica de Yucatán, Unidad de Materiales, Merida, Mexico*

(*Received 2 February 2013; accepted 27 May 2013*)

A non-crimp fabric with a stacking sequence of [0°,+45°,90°,−45°] embedded in epoxy resin matrix was analyzed. Samples for mechanical test were obtained from laminates at different orientations depending on the textile architecture direction at 0°, 45°, and 90° in order to study the relationship between damage initiation and propagation with fabric geometry. Tension mode tests (static and cyclic) were carried out to evaluate the evolution of damage using as a main tool, the acoustic emission technique that allows monitoring the mechanical behavior of the materials during the test in 'real time'. Results show that there is a remarkable mechanical influence of the reinforcement textile in the composite and that damage generation and progression (mechanisms of fracture) is highly dependent of the direction in which the stress is applied in relation with the architecture of the fabric. In static tensile mode, samples at 0° exhibited better mechanical parameters than samples at 90°, while at 45° orientation was lesser. The effect of textile geometry was demonstrated to have an influence in such mechanisms. In cyclic tensile mode, Kaiser effect is observed at low stresses, while the experimental results showed that the Felicity effect became clearer along with the increasing of stress level.

**Keywords:** polymer matrix; mechanical properties; textile architecture; composites; acousticemission

Downloaded by [Renmin University of China] at 11:34 13 October 2013

## 1. Introduction

Composite materials have been used for a long time in various industrial fields such as aeronautic or automotive due to their excellent properties. Nowadays, they are also valorized within buildings and turn to be of current applications as strengthening rods or plates. The new advanced technologies in textile industry have allowed the production of novel fabric geometries used for composites reinforcement in addition to those traditionally produced in the textile market such as woven, non-woven, knitted, or braided. [1–3] Textile composites offer several advantages over unidirectional (UD) composites, such as lower production costs, better drapability, higher delamination, and impact strength.[4–7] However, their mechanical in-plane properties, stiffness, as well as strength, are lower than those of UD-composites. The reason for this drawback is the

*Corresponding author. Email: t-sakai@tmu.ac.jp

© 2013 Japan Society for Composite Materials, Korean Society for Composite Materials and Taylor & Francis

generally higher fiber undulation, which is due to the textile fiber architecture and the fabrication process.[8,9]

The textile architecture poses another challenge on the design process, because different fiber directions are no longer separated, but somehow connected through weaving, braiding, stitching, or knitting. Separate layers with a homogeneous fiber direction as in UD preimpregnated composites are seldom found in textile composites. This kind of textiles is named non-crimp fabrics (NCF) or multiaxial textiles. The description of the geometry of multi-axial multi-ply stitched performs includes the geometry of the stitching yarns and geometry of the fibrous plies.[10] Recently, NCF have gained a place in composite materials manufacture as reinforcement in many structural applications. These textiles consist in two or more layers of UD fibers held together by a secondary non-structural fine additional yarn, commonly of polyester (PES). This holding thread, ideally should not interfere with the mechanical properties, however, it has been demonstrated [4,11,12] that it affects the cracking propagation in the composites. The main fibers can be made of any structural fibers available in any combination. The textile manufacture process allows any orientation in the fibers more complex than that observed in woven (0°/90°). The main problem is that the textile-reinforced composite (TRC) presents very heterogeneous structures. As a consequence, the stress and strain fields within it depend greatly on the constituent's repartition, on their size, and on their spatial arrangement. In other words, it depends on the textile's internal geometry. Hence, a characterization procedure must be able to deal with this geometrical heterogeneity and mechanical anisotropy.[13]

Several test methods and techniques have been developed to evaluate and monitor the damage mechanisms and failure modes. One of these techniques, acoustic emission (AE) has gained fundamental attention in recent years. AE is a non- destructive technique that is capable of passively monitoring failure of a construct with excellent temporal resolution.[14–17] Previous investigations using AE to monitor the integrity of different kinds of fiber reinforcement composite materials have used surface-mounted sensors to identify different signal parameters such as amplitude, energy, etc. and because of more complex damage mechanisms, such as reinforcement (fibers or particulates) failures, delamination, matrix cracking, and debonding of the fiber and matrix, composite materials provide a greater variety of AE sources in fatigue and fracture experiments. AE signals resulting from different damage mechanisms often vary significantly. Furthermore, most of the composites consist of at least one hard or brittle phase, which causes stronger AE signals. The possibility of damage characterization using AE depends on the complexity of textile architecture: the presence of multiple damaged zones can lead to difficult interpretation of AE data. In general, however, most AE can be ascribed to friction or rubbing between damaged parts in the composite.[18] In particular, AE activity during reloading resumes at a fraction of the previously applied load: this fraction is defined as 'Felicity ratio' (FR): FR has been found to be higher for composites with higher residual strength, i.e. less damaged by first loading.[19]

On the other hand, both time and frequency domains contain valuable information for the source and the medium of propagation of AE waveforms. The wavelet transform consists in correlating the analyzed signal with a family of wavelets obtained by dilating an oscillating function of finite duration. In this respect, the wavelet transform acts as a mathematical microscope [4], able to give a quantitative measure of the local appearance of a signal at different scales. The most important outcome in frequency domain is the suggestion that each failure mechanism is distinguished by a different peak frequency of the acquired waveforms. Siron et al. [11] used AE waveform

Downloaded by [Renmin University of China] at 11:34 13 October 2013

Downloaded by [Renmin University of China] at 11:34 13 October 2013

parameters to investigate damage indicators which are related to the physical damage of the composite. Ramirez-Jimenez et al. [12] have applied the frequency method to identify the failure modes in glass/polypropylene composites. The results showed that 100 kHz primary event frequency is due to the fiber/matrix debonding, those between 200 and 300 kHz are due to the fiber slippage and fiber pull-out, and the two higher frequencies appearing in all tests are related to the fiber breaking. Some researchers showed the fiber/matrix debonding is at higher frequency. However, they did not consider the sensors resonant frequency.[20] Ni and Iwamoto [14] concluded that using the time-frequency method of the wavelet transform, the microfailure modes at a fiber breakage and the microfracture mechanism, such as the sequence of each failure mode and their interaction, were clearer. Qi and coworkers [15,16] applied the wavelet transform to analyze AE signals by decomposing the signal into different wavelet levels. Each level represents the components of the decomposed AE signal within a certain frequency range. In this paper, wavelet packet transform method was applied to provide the relevant information from AE signal to discriminate the damage types. It was understood that any signal can be decomposed into a set of wavelet components, each having its specific frequency range. In this paper, AE signals were analyzed using criteria based on the different energy distribution in each component and related a specific failure mode.

## 2. Materials

The material that was studied in this research was a glass-fiber non-crimp fabric (NCF) reinforced epoxy composite. The multiaxial E-glass reinforcement textile (provided by Italian industry Nastrificio Gavazzi) has a mass per unit area of $972 \pm 5\%$ g/m$^2$ and a [0°, +45°, 90°, −45°] stacking sequence; such fabric is classified as quadraxial in accord to the scheme shown in Figure 1. The layers have relative mass fractions as indicated in Table 1 and are stitched together with a PES multifil binding yarn.

The UD fiber bundles in each of the four layers are held together by a fine PES thread in both sides. In the outer layer where fibers are running at 0°, the PES thread is knitted in a zig-zag pattern, whereas in the other side (outer layer at −45°), it is knitted at 0° direction. Figure 2 shows micrographs corresponding to PES threads in both faces, while Figure 3 illustrates both sides details of the multiaxial textile. Here, the zig–zag pattern and the UD yarn of the PES multifil binding yarn can be recognized, as well as

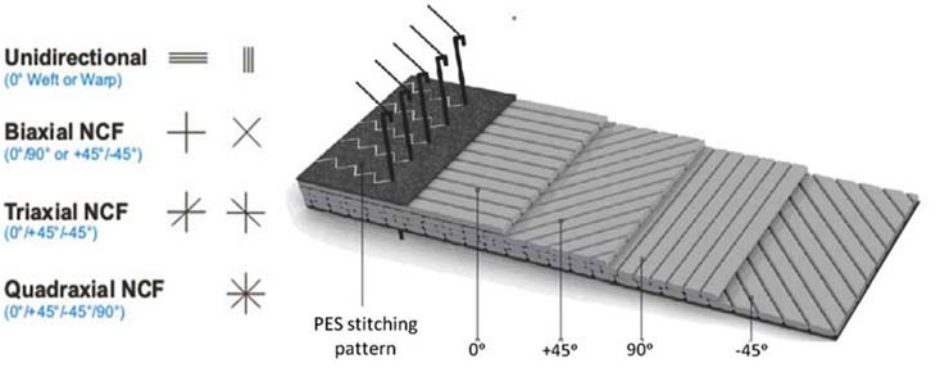


Figure 1. Textile geometry and classification.

Table 1. Textile composition.

| Layer orientation | Weight ($g/m^2$) | Composition |
|---|---|---|
| 0° | 354 | E- Glass |
| +45° | 200 | E- Glass |
| 90° | 207 | E- Glass |
| −45° | 200 | E- Glass |
| Knit yarn | 11 | PES |
| Total | 972 ± 5% | |

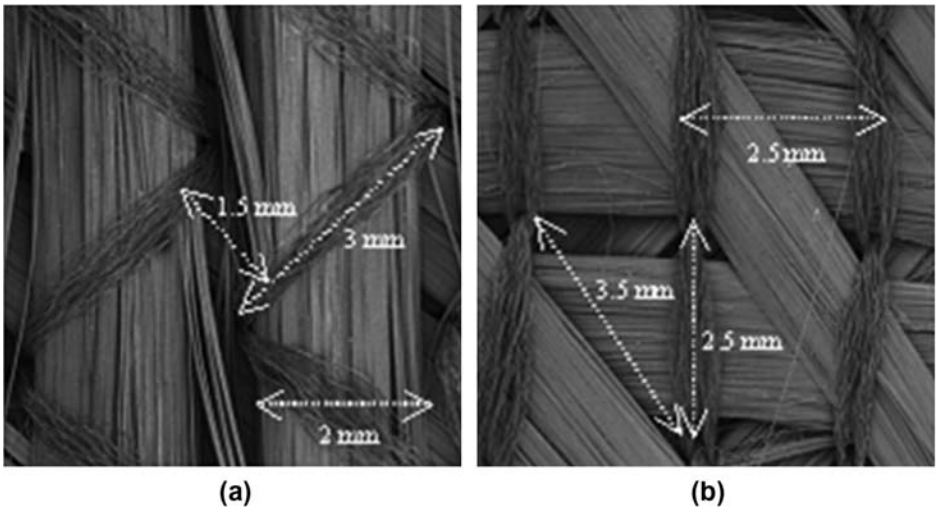


Figure 2. PES knit yarn, (a) zig-zag pattern (b) 0°.

the knots from the stitching. Epoxy system chosen was constituted of resin D.E.R 331 from Dow Company, which is a liquid resin of low viscosity and high content of epoxy groups. The hardener used was 4,4′-diaminodiphenylsulfone (DDS) from Aldrich, which is an aromatic amine with functionality 4, molecular weight 248.3 g/mol, and melting point of 175–177 °C. DDS is a tetrafunctional aromatic amine that provides excellent mechanical properties to the final thermosetting matrix and ensures a good compatibility with the most of the common reinforcements employed in composite materials manufacture.

Figure 4 displays a sketch related to the textile architecture on the PES yarn which is a main factor in the cracking initiation and propagation, as it has been previously observed [4] since transversal knots can act as stress concentrators.

The knots run through the textile thickness acting like pins to hold on the four UD layers. They are considered in the textile architecture as geometrical discontinuities. Under loads, these changes in geometry increase the local stress fields of the composite quite significantly, and they usually represent locations, from which is possible to perform as damage initiation sites. Irregularity of stress distribution at such places means that at certain points, the stress is far above the average value, and under the action of external stresses, progressive failures are likely to start in such way that cracks coalesce joining these points and follow the textile architecture to give the final crack pattern.

Downloaded by [Renmin University of China] at 11:34 13 October 2013

Downloaded by [Renmin University of China] at 11:34 13 October 2013

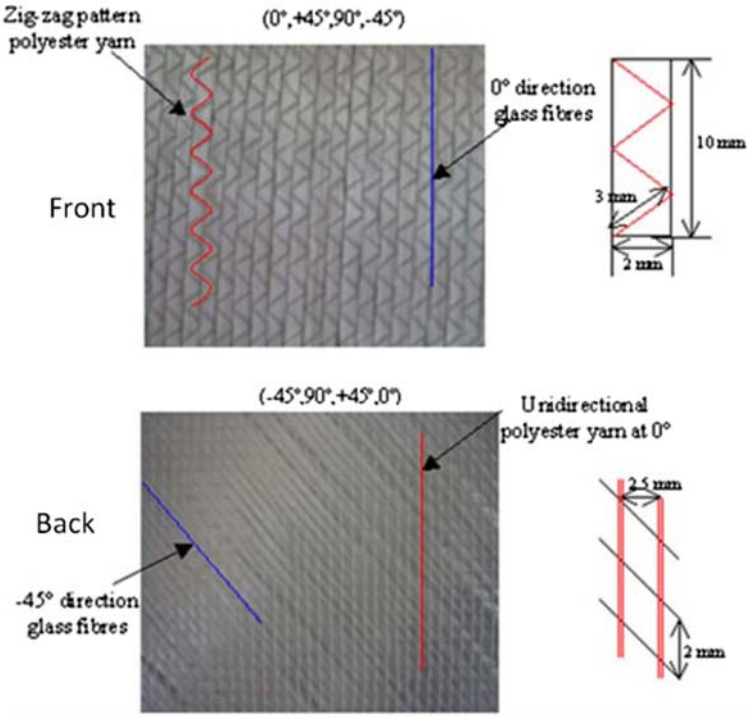


Figure 3. Multiaxial textiles structure, inspection from both sides (Front and Back).

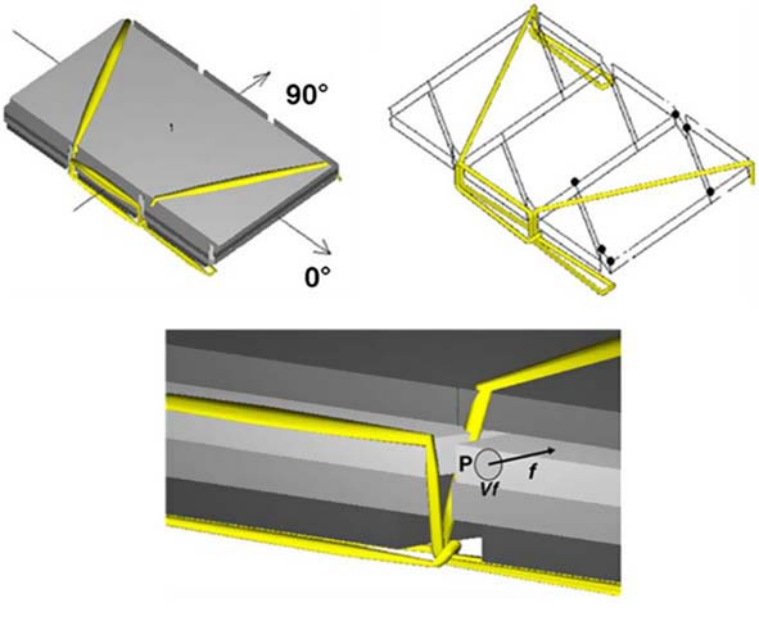


Figure 4. Textile architecture, PES stitch and knots.

Downloaded by [Renmin University of China] at 11:34 13 October 2013

## 3. Experimental procedures

Using one layer of NCF sheet and epoxy resin system as matrix, a composite with a fiber volume fraction of about 18% was manufactured by wet lay-up process. Resin system was placed in a mold and then, the textile was laid in assuring a complete diffusion of the resin in the fabric filaments. The mold was placed in the oven for curing at 140 ° C for 8 h. After this time, the lamina was cooled down to room temperature and finally it was withdrawn from the oven to get the samples for mechanical test. Laminas were elaborated taking into account the three principal direction layers that conform the multiaxial textile (0°, 45°, and 90°). Since +45° and −45° exhibit the same configuration, one set of samples were machinated. Samples were cut from several laminas having each of the four plies of UD fiber orientations (0°, 45°, 90°) aligned to load direction in order to test the effect of the PES knit yarn on the damage initiation and propagation (Figure 5).

A Shimadzu universal machine AG-I 100 KN was used to carry out mechanical tensile tests. All the coupons had a total length of 230 mm, 20 mm width, and an average thickness of 4 mm. Aluminum tabs were placed in both extremes having 50 mm length. The textile direction in question was parallel to load direction in which the samples were loaded to progressively higher strain at a cross-head speed of 0.5 mm/min. Two strain gauges, transversal and longitudinal, were attached in the center of the sample in order to obtain the mechanical parameters in both directions. The stress–time curves were obtained and the mechanical parameters such as Young′s modulus ($E$) and stress ($\sigma$) at failure were determined. Young's modulus were calculated using the stress–strain diagram until the strain value as 0.2%, however, the strain gage fractured before the final failure, therefore, the stress–time diagrams are used in this paper. AE piezoelectric sensors were attached to the sample as shown in Figure 6 to obtain the signal in order to be related to damage development and mechanisms of fracture. Two tensile mode tests were carried out for each sample: static, which consists in loading the material to a constant cross-head speed all the way until fracture occurs; and the cyclic mode that consists in loading the materials to a certain stress values preceded by unloading to zero stress and then loading again passing the previous stress value to a higher stress level and so on. Cyclic mode, also called dynamic mode, was carried out at different stress values and was monitored by the AE, and those tests were continued until total fracture of the materials sample. By these means, the correlation of the stress–time curve with the acoustic signal (events) provided information about the damage magnitude through

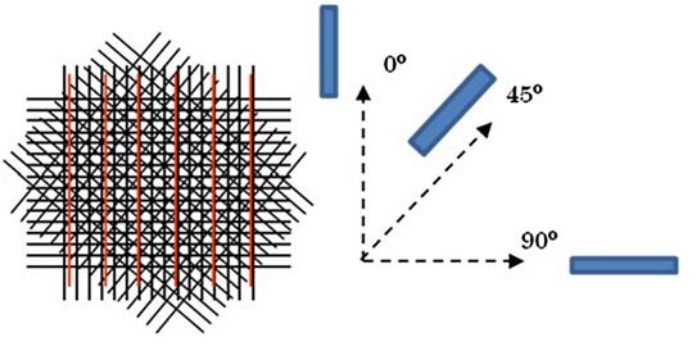


Figure 5. Samples for mechanical testing orientation.

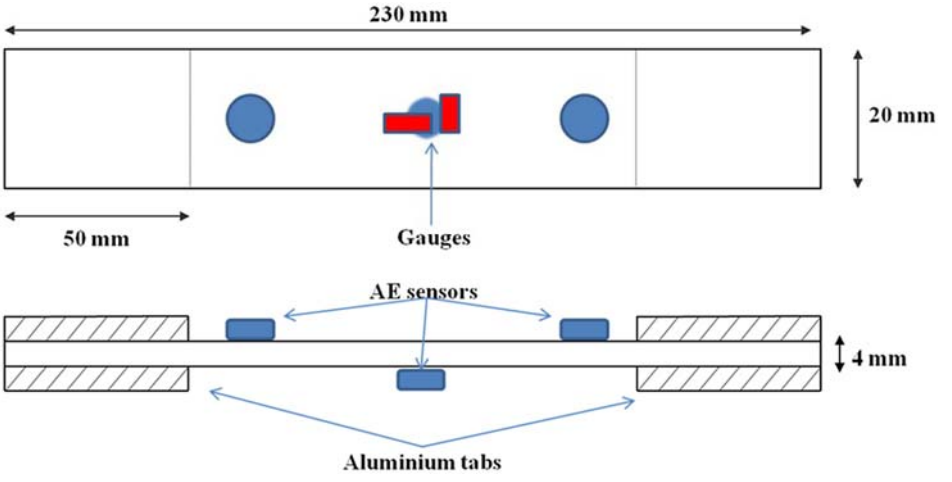


Figure 6. Sample dimensions and AE sensors locations.

the Felicity effect analysis. Unlike Kaiser Effect in which AEs are not observed during the reloading of a material until the stress exceeds its previous high value, in Felicity Effect, the presence of AE is detectable at a fixed predetermined sensitivity level at stress levels below those previously applied. Insignificant flaws tend to be shown by the Kaiser effect, while significant flaws, related to a certain degree of damage, tend to be exhibited by the Felicity effect.

Transparency of the composite samples allowed visual monitoring of the damage development with a fixed camera (Figure 7). Information data obtained were saved and processed to exhibit the corresponding values. In addition, due to an unusually small difference in the indices of optical refraction of the matrix-system and the glass-fibers, the obtained samples showed an extraordinary transparency, therefore, matrix cracks, voids, and inclusions could easily be detected by transmitted light photography. The glass fibers cannot be seen, while the binding yarns remain visible.

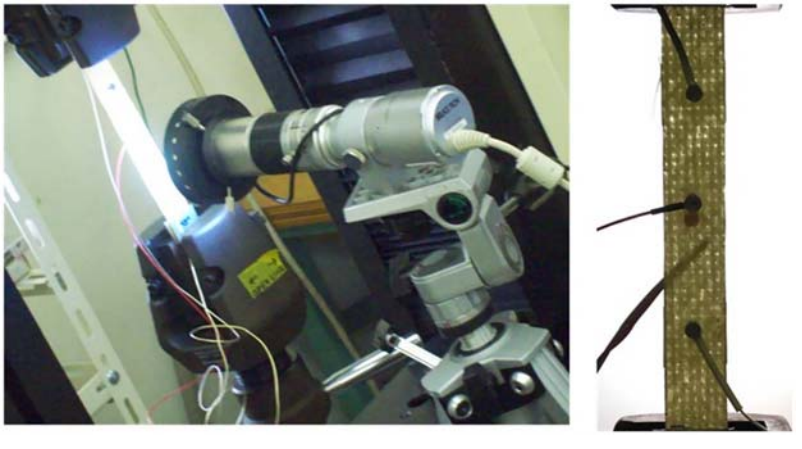

Figure 7. Textile composite sample in tension test.

Downloaded by [Renmin University of China] at 11:34 13 October 2013

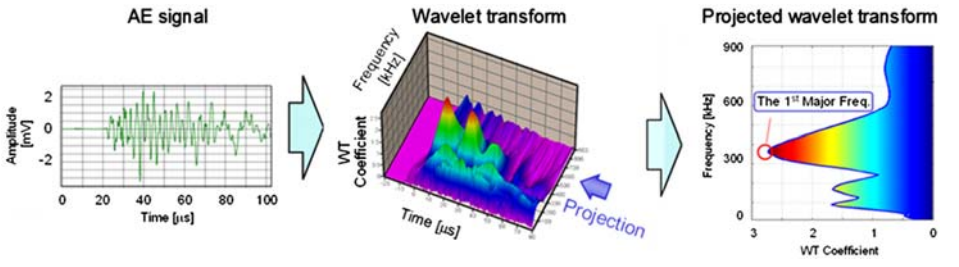


Figure 8. Schematic drawing of the projected wavelet transform.

Downloaded by [Renmin University of China] at 11:34 13 October 2013

During the test, AE signals were monitored by three wide-band AE sensors (NF Corporation, AE-900M). One sensor was attached at the center of the gauge length. The others were attached at the edge of gauge length and used as guard sensors, by which mechanical noises from testing apparatus were detected earlier than the central sensor; thereby they could be discriminated from the AE signals due to microdamages. The AE signals were amplified by 40 dB and the threshold level was set to the value of 26.8 dB at the input of the sensors. The AE signals were processed by an AE analyzer (Vallen Systems, AMSYS-5). The threshold for the AE equipment was established by performing preliminary analysis in order to be able to record the AE signals from the tests without spurious noise. Optical microscopy was used to analyze and identify the cracking initiation sites and to relate them to the architecture of the knitted textile. For the analysis of waveforms, MATLAB software has been chosen since it has wavelet toolbox with numerous options and it is possible to create codes according to the application field. By this technique, we can improve the relationship between the failure modes and the corresponding frequency range. In this study, projected wavelet transform (PWT) analysis is adopted to classify the AE signals. The analysis yields the characterization of AE signals in terms of transient frequency component. Figure 8 illustrates the procedure of the PWT analysis. Analyzing frequency at the peak wavelet coefficient, which indicates strength at given times and frequencies in a signal, the first major frequency of each AE signal is extracted.

## 4. Results and discussion

All manufactured composites appeared to be of a homogeneous good quality and surface finish; the procedure did not lead to any detrimental effects on either processability or general product appearance. Samples were cut from several laminas having each of the four plies (+45 and −45 are geometrically similar) of UD fiber orientations (0°, 45°, and 90°) aligned to load direction in order to test the effect of the PES knit yarn on the damage initiation and propagation.

### *4.1. Static mode*

Five samples were tested for each angular orientation. The mechanical behavior tendency was observed to be as shown in Figure 9, where typical stress–time curves for one of each angular sample (0°, 45°, 90°) are plotted as representative.

In each curve, it is possible to appreciate several discontinuities that are related to significant cracking development transversally to the sample. Immediately after the first

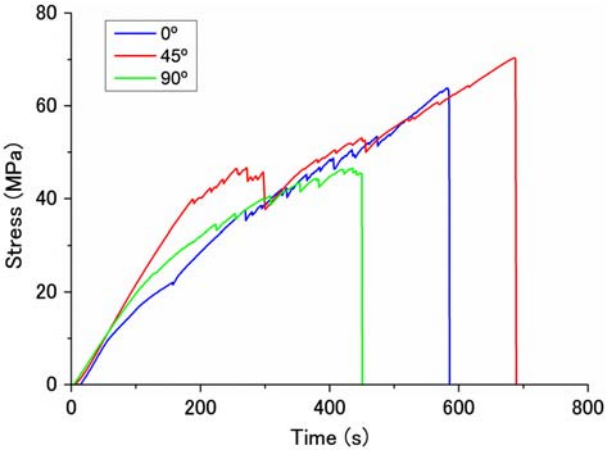


Figure 9. Stress vs. time curve for textile-reinforced composites.

cracks appear, a 'knee' becomes visible in the stress–time curve. At higher strain, discontinuities are more frequent, the higher the load, the more cracks are formed. Samples at 0° exhibited slightly higher mechanical parameters and resistance to the damage development. Samples at 90° showed the lowest mechanical parameters since they exhibited the major crack density (amount of crack per area) transversally along the sample. Enhanced Young modulus and maximum tensile stress (UTS) were displayed by samples at 0° direction, whereas at 45° and 90° there is not a significant variation in this behavior (Table 2). This consistency has been analyzed in previous investigations [4] and the tendency is similar.

The proximity of the mechanical parameter values obtained in all the orientations despite the PES knit yarn direction and the fiber density between each layer is noticeable. Although slightly dispersion was obtained in its values, it appears that the better mechanical behavior was exhibited by the 0° material. Apparently, textile geometry (stacking sequence) does not affect significantly the mechanical parameters values; however, damage development and propagation along samples depending on the loading direction are influenced by the PES knit yarn structure.

The Stress (MPa)–time (s)–amplitude curves for samples when the textile is oriented at 0° is presented in Figure 10. AE signal detected over 280 s are intimately related to the first deflection in the curve, which is also correlated to the appearance of the first significant damage that emits high energy. This damage is associated to matrix cracking in the composite.

Table 2. Mechanical parameters for textile reinforced composites: (a) actual data, (b) [4].

| | (a) | | (b) | |
|---|---|---|---|---|
| | E (GPa) | UTS (MPa) | E (GPa) | UTS (MPa) |
| 0° | 4.4 | 64 | 4.1 | 66 |
| 45° | 2.7 | 59 | 3.4 | 58 |
| 90° | 3.1 | 53 | 4.3 | 59 |

Downloaded by [Renmin University of China] at 11:34 13 October 2013

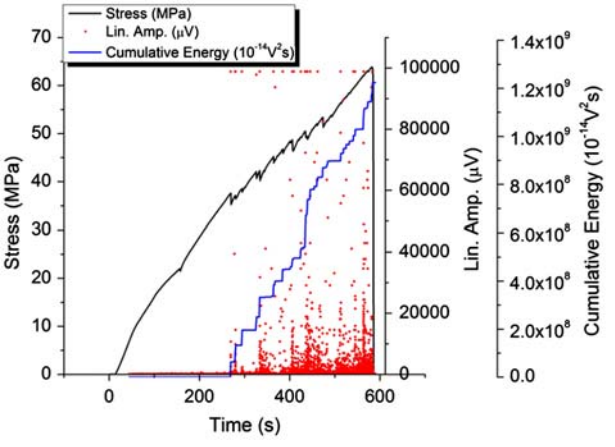


Figure 10. AE signal behavior in composites at 0°.

Recording by the AE sensors in PWT is shown in Figure 11 for samples at 0° where significant wavelet transform coefficient (WTC) can be appreciated at around 400 s, which is related with the increment of damage, to the end of the test at about 550 s due to the progress of damage near total failure. Frequencies were found to be detected in an interval from 150 to 250 kHz in early stage (from 280 to 500 s). As a result of observation with microscope, it was assumed that these frequencies are corresponded to the matrix cracking in the composites. And then (after 500 s), frequencies were found in the range of 400 kHz–800 kHz. These frequencies are corresponded to the fiber-matrix interface delamination.

For samples at 45°, the curves along AE signals are represented in Figure 12. For this case, main damage is noticed slightly lower than previous sample (0°), at about 230 s, and it was also perceived that the curve contains more discontinuities since this sample showed more damage in the form of matrix cracking than at 0°. Higher amount of damage is the reason the energy curve is raising more rapidly.

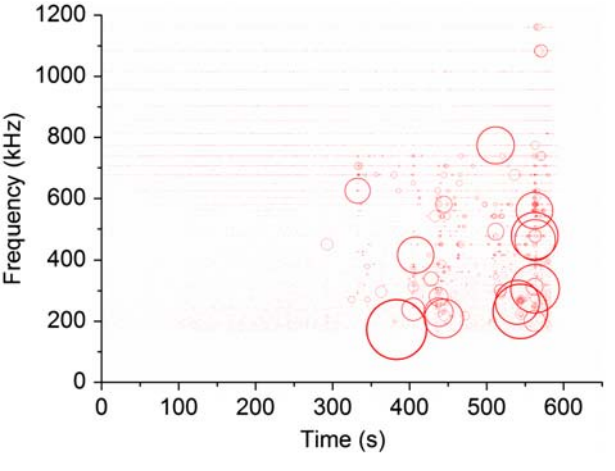


Figure 11. AE signal wavelet transform for samples at 0°.

Downloaded by [Renmin University of China] at 11:34 13 October 2013

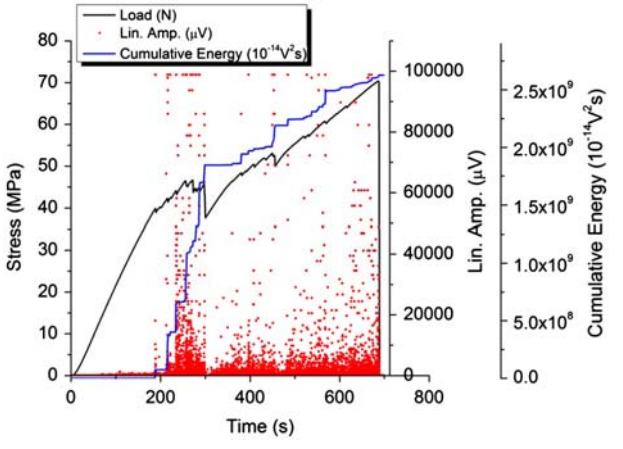


Figure 12. AE signal behavior in composites at 45°.

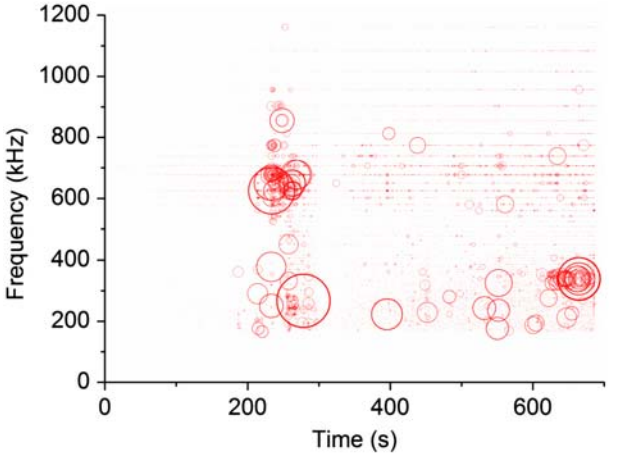


Figure 13. AE signal wavelet transform for samples at 45°.

Figure 13 shows the wavelet transform information obtained from the AE sensors. It is noticeable that significant WTC are found from the beginning of the main damage is detected around 250 s. As shown in this result, this can be correlated to the matrix cracking and the fiber-matrix interface delamination. Once the delamination occurred, the failure mode changed to matrix cracking and friction between fiber and matrix after 300 s. The frequencies range from 300 to 400 kHz is associated to the friction between fiber and matrix.

Finally at 90° directions, the curve is presented in Figure 14 where it is possible to observe more small discontinuities related with the AE signals identified as matrix cracking. As observed previously at 45°, energy is augmented rapidly as more cracking damage occurs. In all the samples tested in tension (0°, 45°, and 90°), no fiber breakage was observed or AE detected until total fracture happened. Samples at 90° exhibited an early damage development in comparison with the other orientations. They presented a

Downloaded by [Renmin University of China] at 11:34 13 October 2013

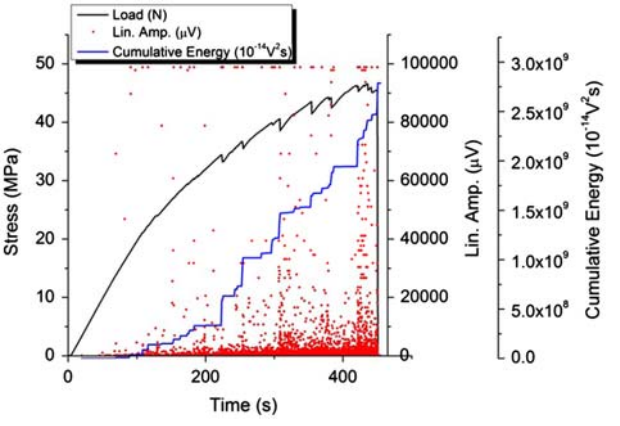


Figure 14. AE signal behavior in composites at 90°.

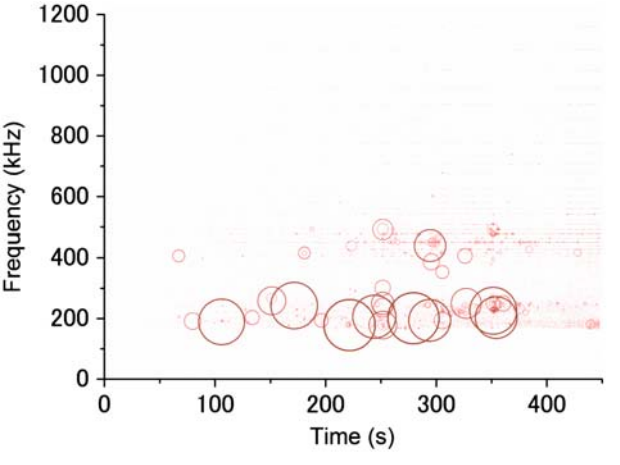


Figure 15. AE signal wavelet transform for samples at 90°.

higher cracking density, which is the amount of cracks per area. For this material, mechanical behavior was observed to show the lowest resistance due to the orientation of the reinforcing non-crimp textile geometry with respect to the applied tensile load that allows transversal matrix cracks to develop along the coupon.

Figure 15 shows the frequency time data obtained from the AE sensors for 90° orientation. Low frequency waves are detected primarily at about 200 kHz, indicating a quick and sudden damage development. Higher frequencies were detected in fewer events with small WTC.

### *4.2. Cyclic mode*

Textile-reinforced composites were tested on cyclic tensile mode, samples were loaded at a certain stress value and, at this point, the applied load is released. By this means, damage accumulation in the materials can be identified by observing two inherent phe-

Downloaded by [Renmin University of China] at 11:34 13 October 2013

Downloaded by [Renmin University of China] at 11:34 13 October 2013

nomena: Kaiser and Felicity effects, which are parameters of damage evolution. Kaiser effect is observed in most metals, in which AEs are not observed during the reloading of a material until the stress exceeds its previous high value. Dunegan corollary [21] states that if AE is observed prior to a previous maximum load, some type of new damage has occurred, therefore, Felicity effect is used to analyze this type of damage. Felicity effect is related to the presence of AE, detectable at a fixed predetermined sensitivity level at stress levels below those previously applied.

Stress–time–amplitude curve is displayed in Figure 16 for a composite sample at 0° direction. Five cycles were selected in order to observe the AE signals to be related with the curve. The first cycle was taken at low strains in the elastic region, so no signals are recorded. Second one did not detect any significant signal neither indicating that no damage has yet started. Third cycle between 230 and 560 s, AE signals were detected after previous load value was reached (A) indicating the initiation of damage. At this point, when the load is released few small signals are detected during unloading which is related to a minimal damage (B). In next cycle (fourth), AE is perceived again after the previous stress value is reached (B), no damage was observable during loading, but at unloading, more signals were detected indicating additional damage (C). Finally, during the loading of the last cycle, small AE signals are obtained just before the last stress value has been reached indicating major damage development (C). At this stage, the waves are more intense due the proximity of fracture.

Figure 17 shows the results for a composite at 45° direction that was loaded–unloaded in four cycles. First cycle was carried out a low strains in the elastic region and as a result, no AE signals are presented (A). Second one does not display any significant AE signals although plastic deformation starts to take place (B), however, very small indication of microdamage is detected by the sensors around 150 s. In the third cycle, significant AE signals are detected after the previous stress value has been reached (B). Since the damage development is elevated at higher strains after 450 s, when the sample is released from the applied load, at the beginning of the unloading, some additional AE waves are observed (C). It is until the final cycle when Felicity effect is detected due to the evolution of damage; AE signals are detected before the previous stress value is reached. At the end, the sample is totally fractured.

The mechanical behavior for composite samples oriented at 90° is displayed in Figure 18. In this case, five cycles were obtained from the tensile test. First one is related

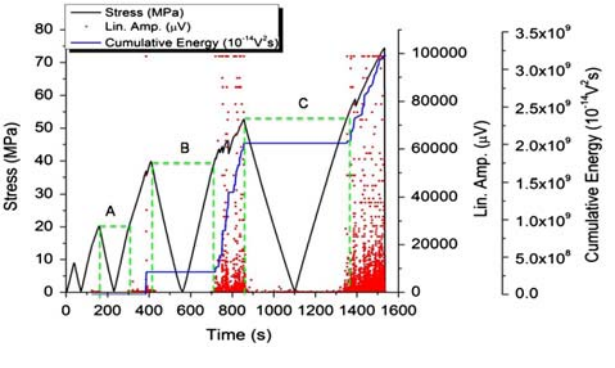


Figure 16. AE signal behavior in composites at 0° in cycle test.

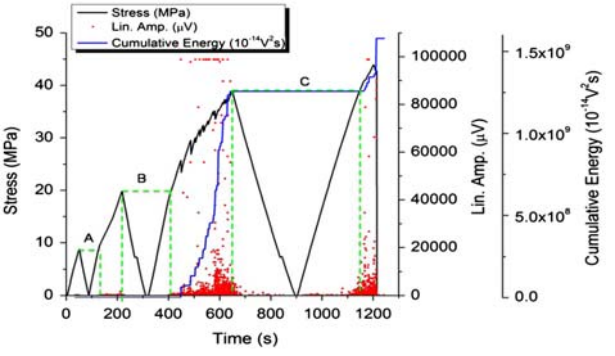


Figure 17. AE signal behavior in composites at 45° in cycle test.

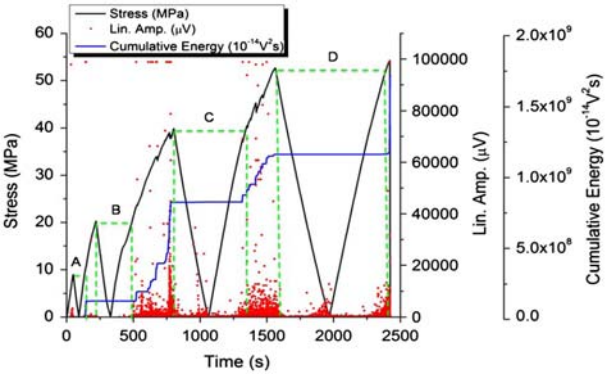


Figure 18. AE signal behavior in composites at 90° in cycle test.

to elastic region which was observed to be too small, since some AE signals related to predamage are detected around 90 s in agreement with damage initiation detected in Figure 14 for similar material in static tensile mode (A). Second cycle shows small AE detection when the previous stress value is reached probably due to microdamage associate to fiber/matrix interphase debonding (B). In the third cycle (B), small signals are detected before previous stress has been reached and a discontinuity appears in the curve indicating an initiation of significant damage in the material (matrix cracking), so Felicity effect is observed in early stages. Increment of damage is notorious when load applied is released and waves are registered during unloading (C). Consequently, when strain is higher (fourth cycle) AE waves, are detected before the previous load has been achieved indicating a damage development in the matrix phase (C) and Felicity effect becomes clearer. Again, when the material is unloaded, signals are detected in compression (D). Finally, at the end of the test prior to fracture, AE is detected again before reaching the previous load value, making evident the high amount of damage developed during the tensile test.

Samples fractured after static tensile mode are presented in Figure 19. The probable mechanisms of failure observed during tensile loading for the multiaxial reinforced composite material follows the subsequent stages:

Downloaded by [Renmin University of China] at 11:34 13 October 2013

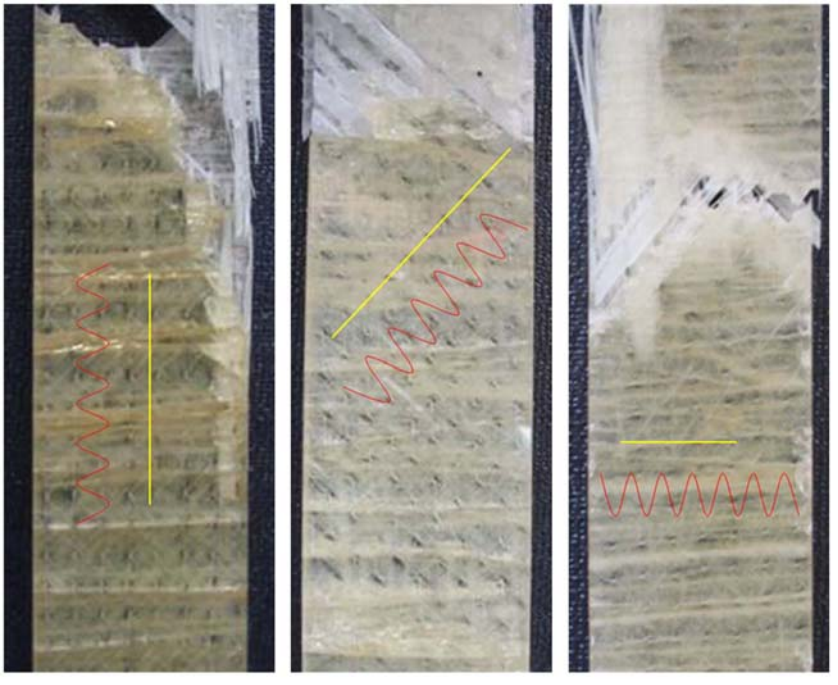


Figure 19. Crack development on tensile mode samples, yellow and red lines indicate UD and zig-zag PES thread pattern, respectively. (a) sample tested at 0°, (b) sample tested at 45°, and (c) sample tested at 90° [4].

(1) Textile fibers oriented transversally to load direction are the first in exhibiting damage initiation in the interfacial region by a fiber/matrix interface debonding, specially in points were stress magnification is higher; in this case, this would be the peaks of the zig-zag PES yarn and the knots from the stitching to join the textile strands in the UD PES thread (in both faces of the composite).
(2) Fibers oriented at 0° support the most of the load (UD parallel to applied stress), consequently load generates damage initiation in fibers oriented as +45° and −45°
(3) At higher stress, cracks parallel to 0° fibers appear due to interplanar tension. At this point, matrix cracking occurs. Damage is significant and the material is near to fracture.
(4) Finally, fiber breakage takes place and the material fails definitively.

## 5. Conclusions

The goal of the present study was to characterize the mechanical behavior of a (NCF)-epoxy composite by using a non-destructive technique such as AE in order to correlate the acoustic waves with the onset of crack and development of failure until total fracture of the sample. Mechanical behavior of textile composite materials is highly dependent on the direction in which the stress is applied in relation with the architecture

Downloaded by [Renmin University of China] at 11:34 13 October 2013

of the fabric. Damage cracking development is influenced by the PES thread (zig-zag and UD). Kaiser effect is observed at low stresses, while the experimental results showed that the Felicity effect became clearer along with the increasing of stress level. Each loading cycle would cause new damage inside the material, and the response of material to the new loading cycle is different from the previous cycle. AE signals detected during felicity effect are due to the damage induced in the material at the interphase area which generates friction between the fibers and matrix. From the results obtained by tensile testing, it becomes clear that AE is a powerful tool to detect the onset of cracking within composite materials earlier than by other methods. Selection and classification of AE signals on the basis of stress–time curve allows a distinction of failure mechanisms on textile-reinforced composites such as matrix cracking, fiber breaks, and interfacial failure (fiber/matrix debonding, fiber pull-out). Therefore, a signal by signal classification of AE sources permits the evaluation of damage stages on the basis of failure mechanisms.

Downloaded by [Renmin University of China] at 11:34 13 October 2013

## References

[1] Donald S, Mansour M. 3D woven composites: cost and performance viability in commercial applications, 48th International SAMPE Symposium, Long Beach, CA, USA.
[2] Cox BN, Davis JB. Braided composites for energy absorption under tensile loading. J. Mater. Sci. 2000;35:3467–3478.
[3] Parameshwaranpillai T, Lakshminarayanan PR, Nageswara Rao B. Taguchi's approach to examine the effect of drilling induced damage on the notched tensile strength of woven GFR–epoxy composites. Adv. Compos. Mater. 2011;20:261–275.
[4] Cruz-Santos G, Rodriguez-Laviada J, Rios-Soberanis CR. Damage development in a noncrimp-glass fabric reinforced epoxy composite material. Polym. Compos. 2009;30:1800–1808.
[5] Saito H, Kimpara I. Evaluation of impact damage mechanism of multi-axial stitched CFRP laminate. Composites: Part A. 2006;37:2226–2235.
[6] Zhang Y, Huang Z-M, Ramakrishna S. Tensile behaviour of multilayer knitted fabric composites with different stacking configuration. Appl. Compos. Mater. 2001;8:279–295.
[7] Leong KH, Ramakrishna S, Bibo GA, Huang ZM. The potential of knitting for engineering composites – a review. Composites A. 2000;31:197–220.
[8] Ramakrishna S, Hamada H, Rydin R, Chou TW. Impact damage resistance of knitted glass fiber fabric reinforced polypropylene composite laminates. Sci. Eng. Compos. Mater. 1995;4 (2):61–72.
[9] Loendersloot R, Lomov SV, Akkerman R, Verpoest I. Carbon composites based on multiaxial multiply stitched preforms. Part V: geometry of sheared biaxial fabrics. Composites: Part A. 2006;37:103–113.
[10] Beier U, Fischer F, Sandler JKW, Altstadt V, Weimer C, Buchs W. Mechanical performance of carbon fibre-reinforced composites based on stitched performs. Composites: Part A. 2007;38:1655–1663.
[11] Siron O, Chollon G, Tsuda H, Yamauchi H, Maeda K, Kosaka K. Microstructural and mechanical properties of filler-added coal-tar pitch-based C/C composites: the damage and fracture process in correlation with AE waveform parameters. Carbon 2001;39:2065–2075.
[12] Ramirez Jimenez CR, Papadakis N, Reynolds N, Gan TH, Purnell P, Pharaoh M. Identification of failure modes in glass/polypropylene composites by means of the primary frequency content of the acoustic emission event. Compos. Sci. Technol. 2004;64:1819–1827.
[13] Eitzen DG, Wadley HNG. Acoustic emission: establishing the fundamentals. J. Res. Nat. Bur. Stand. 1984;89:75–100.
[14] Ni Q-Q, Iwanto M. Wavelet transform of acoustic emission signals in failure of model composites. Eng. Fract. Mech. 2002;69:717–728.
[15] Qi G, Barhorst A, Hashemi J, Kamala G. Discrete wavelet decomposition of acoustic emission signals from carbon-fiber-reinforced composites. Compos. Sci. Technol. 1997;57:389–403.

[16] Qi G. Wavelet-based AE characterization of composite materials. NDT&E Int. 1997;33: 133–144.
[17] Park J-M, Kim P-G, Wang Z-J, Kwon D-J, Lawrence De vries K. Interfacial evaluation and self-sensing of single micro-carbon fiber/CNF–brittle- cement composites using electro-micromechanical tests and acoustic emission. Adv. Compos. Mater. 2011;20:149–168.
[18] Hamstad MA, Downs KS. On characterization and location of acoustic emission sources in real size composite structures: a waveform study. J. Acoust. Emission 1995;13:S1–S59.
[19] Hamstad MA. A review: acoustic emission as a tool for composite materials studies. Exp. Mech. 1986;26:7–13.
[20] Arumugam V, Kumar S, Santulli C, Sarasini F, Stanley AJ. A global method for the identification of failure modes in fibreglass using acoustic emission. J. Test. Eval. 2011;39:103730.
[21] Dunegan H, Harris D, Tetelman A. Detection of fatigue crack growth by acoustic emission techniques. Mater. Eval. 1970;28:221–227.

Downloaded by [Renmin University of China] at 11:34 13 October 2013